Nuclear Instruments and Methods in Physics Research A 614 (2010) 278–286

Contents lists available at ScienceDirect

Nuclear Instruments and Methods in Physics Research A

journal homepage: www.elsevier.com/locate/nima

Superheated droplet detector response to fabrication variations

M. Felizardo [a,b,c,*], T. Morlat [b], T.A. Girard [b], R.C. Martins [c], A.R. Ramos [a,b], J.G. Marques [a,b]

[a] Instituto Tecnológico e Nuclear, Estrada Nacional 10, 2686-953 Sacavém, Portugal
[b] Centro de Física Nuclear, Universidade de Lisboa, 1649-003 Lisbon, Portugal
[c] Instituto de Telecomunicações, IST, Av. Rovisco Pais 1, 1049-001 Lisbon, Portugal

ARTICLE INFO

Article history:
Received 14 October 2009
Received in revised form
27 November 2009
Accepted 5 December 2009
Available online 16 December 2009

Keywords:
Superheated droplet detectors
Instrumentation

ABSTRACT

Constructions of superheated droplet detectors (SDDs) are easily (and sometimes unavoidably) altered in the fabrication process by small variations in the ingredient concentrations and fractionating of the superheated liquid. The devices have moreover been stored at temperatures below 0 °C prior to usage in order to de-sensitize their response during transport. We report studies of the response differences of high concentration SDDs with respect to variations common to their fabrication, to include ageing, concentration, gel stiffness, and droplet size.

1. Introduction

A superheated droplet detector (SDD) consists [1] of a uniform dispersion of micrometric-sized halocarbon superheated liquid droplets suspended in a hydrogenated gel. Energy deposition by irradiation triggers the phase transition of the superheated droplets, generating millimetric-sized bubbles [2] which can be recorded by either visual, chemical, or acoustic means. SDDs have been used in neutron dosimetry for over a decade [3,4]; more recent applications include neutron spectrometry [5,6], and dark matter detection [7,8].

The physics underlying the SDD operation is described in detail in Ref. [9]; we here provide only a short description. The superheated droplets share the same working principle as bubble chambers, with the significant difference being that SDDs are continuously sensitive since the droplet population can be maintained in steady-state superheated conditions (i.e., above its boiling point), whereas in the bubble chamber the liquid is only sensitized for brief periods of time. Two conditions are required for the nucleation of the gas phase by energy deposition in the superheated liquid [10]: (i) the energy deposited must be greater than a thermodynamic minimum, and (ii) this energy must be deposited within a minimum thermodynamic distance inside the droplet. Both conditions depend on the refrigerant and its thermodynamic degree of superheating: typically the higher the superheat of the droplets, the lower the energy required for bubble nucleation, i.e., the lower is the threshold energy of the detector.

Generally, studies of SDD response have been confined to low concentration devices, and have confirmed the essential underlying physics of the SDD [11–14]. These have been generally based on polyacrylamide gels. The PICASSO dark matter project has provided similar confirmations with their devices of 0.5–1% concentrations [15], also based on polyacrylamide gels. The SIMPLE dark matter detectors in contrast are generally of 1–4% concentrations, fabricated from food gels. Fig. 1 shows a picture of the SIMPLE dark matter detector with its capping: the microphone is seen below, with the cable interface vertical; the horizontal coupling permits over-pressuring of the device up to 4 bar.

The SDD constructions are easily (and sometimes unavoidably) altered in the fabrication process by small variations in the ingredient concentrations and fractionating of the superheated liquid, which might also alter their construction characteristics and hence the device performance. We here describe studies of the influence of these fabrication variations and cold storage on the detector response. Section 2 describes the experimental disposition. Section 3 provides an analysis of the results of variations in the ageing, detector concentration, gel stiffness, and droplet size with variation in the operating temperature. The results are discussed and conclusions are given in Section 5.

2. Methodology and instrumentation

The normal standard test detector (150 ml) is a scaled down version of the 1 l SIMPLE dark matter SDD, with a uniform dispersion of a few grams of superheated droplets of R-12 (CCl_2F_2)

* Corresponding author at: Instituto Tecnológico e Nuclear, Estrada Nacional 10, 2686-953 Sacavém, Portugal.
E-mail address: felizardo@itn.pt (M. Felizardo).

0168-9002/$ - see front matter © 2009 Elsevier B.V. All rights reserved.
doi:10.1016/j.nima.2009.12.025

Fig. 1. SIMPLE detector and its instrumented cap, showing the microphone interface (vertical) and pressure couple (horizontal).

instead of R-115 (C_2ClF_5). The droplets are suspended in a hydrogenated gel matrix composed of glycerin (78.52%), gelatin (1.76%), bi-distilled water (16.10%) and polyvinylpyrrolidone—PVP (3.62%).

The gel itself is formed by combining powdered gelatin and bi-distilled water with slow agitation to homogenize the solution. Separately, PVP is added to bi-distilled water, and agitated at 60 °C. The glycerin solution is then slowly added to the gel in a detector bottle. Following outgassing and foam aspiration, the solution is left overnight at 48 °C with slow agitation to prevent air bubble formation.

The detector bottle is then removed to a stirrer/hotplate within a hyperbaric chamber, and the pressure raised to just beyond the vapor pressure at 45 °C. After thermalization, the agitation is stopped and the refrigerant injected into the gel. The pressure is then quickly raised to 19 bar to prevent the droplets from rising to the surface, and a rapid agitation initiated to shear big droplets; simultaneously, the temperature is raised to 45 °C to create a temperature gradient inside the matrix and permit dispersion of the droplets. After 30 min, the temperature is slightly reduced for 5 h (with pressure and agitation unchanged). The refrigerant, in liquid state, is divided into smaller droplets by the continued agitation. Finally, the heating is stopped: the temperature is decreased until the sol–gel transition is crossed, during which the stirring is reduced and finally stopped. The droplet suspension is quickly cooled to 15 °C and left to set for 40 min, then cooled to 5 °C where it is maintained for ~15 h. The pressure is then slowly reduced to atmospheric pressure, and the detector removed to cold storage or utilization. The process results in approximately uniform and homogeneous (30 ± 15 μm diameter) droplet distributions, as determined by optical microscopy. Longer fractionating times give smaller droplet diameters; shorter times, larger diameters.

Data on bubble nucleation was obtained acoustically, using the developed instrumentation [16]. The acoustic shock wave associated with the rapid bubble expansion following a nucleation event is sensed by an electret microphone cartridge (MCE-200) with a frequency range of 20 Hz–16 kHz (3 dB), SNR of 58 dB and a sensitivity of 7.9 mV/Pa at 1 kHz, ensheathed in a protective latex covering and installed inside the detector container within a glycerin layer above the droplet suspension. The microphone output is amplified by a high gain, low noise, digitally controlled microphone preamplifier (Texas Instruments PGA2500), which is directly coupled to the input of an acquisition channel. This system provides a noise level of 10 mV, permitting the discrimination of all acoustic backgrounds common to the measurements via fast Fourier transform (FFT) analyses [16]. Data was acquired in Matlab files of ~5 MB each at a constant rate of 32 kSps for periods of 5 min each.

The detectors were placed in a water bath with its temperature controlled by a stainless steel pt1000 probe [H62IKA]. The bath was located inside an acoustic foam cage, constructed for the purpose of environmental noise reduction. Previous studies have shown the CCl_2F_2 device insensitive to γ's, cosmics and minimum ionizing radiations below a reduced superheating of $s=(T-T_b)/(T_c-T_b)\sim 0.5$ [17], where T, T_b and T_c are the operating, boiling and critical temperatures at a given pressure, corresponding to 41 °C; the gel is observed to begin melting at ~35 °C. Since the SDD sensitivity increases with temperature, the measurements were performed over the range of 15–30 °C in steps of 5 °C. Each temperature measurement required a stabilization time of about 30 min. The temperature of each detector was measured with a type k thermocouple [RS 219–4450].

Figs. 2 and 3 show a typical bubble nucleation event and its frequency spectrum obtained with a standard test device. The FFT

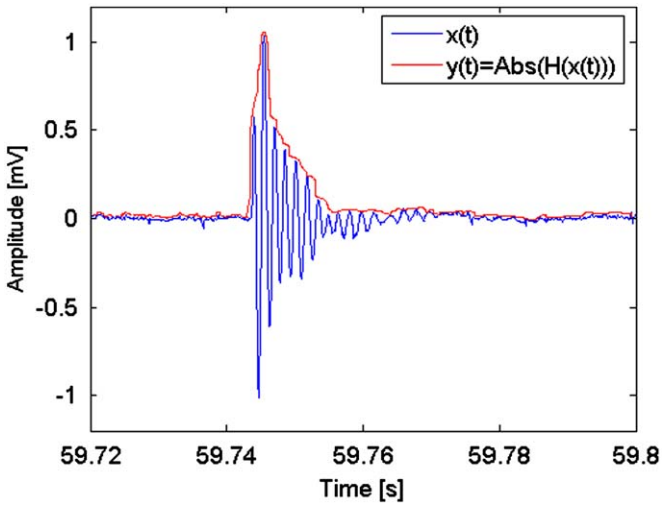

Fig. 2. Typical pulse shape of a bubble nucleation event.

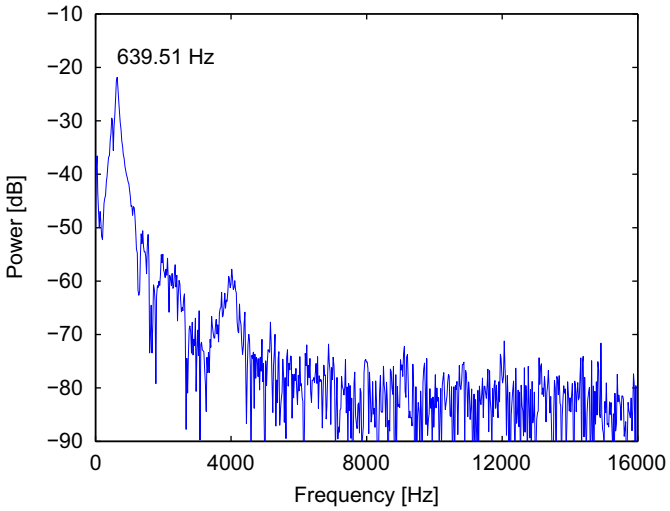

Fig. 3. Fast Fourier transform of the event in Fig. 2.

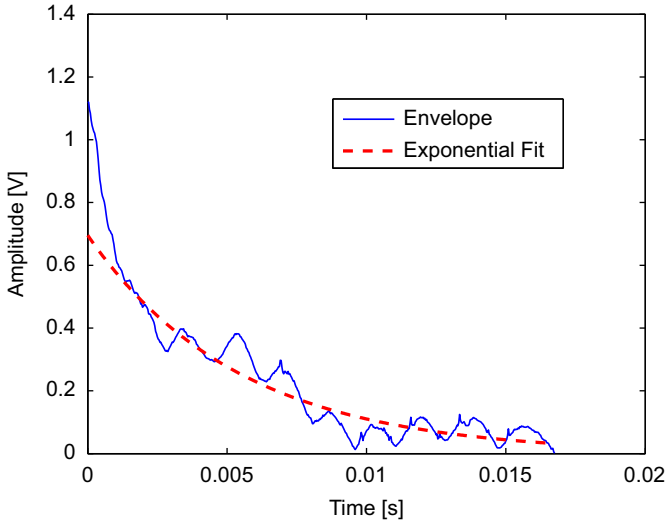

Fig. 4. Best fit to an exponential function of the amplitude envelope from the pulse shown in Fig. 2, with $\tau \sim 20$ ms.

is characterized by a peak at ~640 Hz, with some lower power harmonics around 2 and 4 kHz. As in Ref. [5], the nucleation events were generally stimulated by environmental radiations. These were cross-checked against events generated by irradiating the detectors using a quasi-monochromatic 54 keV neutron beam obtained with a Si+S passive filter at the Portuguese Research Reactor [18].

The data files were first filtered using a pulse shape validation routine [19], which sets an amplitude threshold, identifies the beginning and end of each spike based on the previous threshold, amplitude-demodulates the time evolution of the spike, measures the decay time constant (τ) of the pulse and finally suppresses pulses exhibiting τ's below a selected threshold. As seen in Fig. 4, the best fit to the exponential function of the amplitude envelope from the pulse shown in Fig. 2 gives $\tau \sim 20$ ms. An efficiency of 100% was obtained with a τ window of 10–40 ms.

The common acoustic backgrounds have been found to be fractures of the gel, trapped N_2 gas in the gel and microleaks intrinsic to SDD fabrication and operation. These background events have been well characterized in terms of their time constants and frequencies, as shown in Table 1, and are easily discriminated from true nucleation events via their power spectrum analysis [16].

Table 1
Comparison of the characteristics of several common acoustic backgrounds with those of a true nucleation event [16].

Event type	Time constant (ms)	Principal frequency (Hz)
Microleaks	17	2800–3500
Fractures	36	34
Trapped N_2	91	40
True nucleation event	10–40	450–750

3. Results (SDD parameter variations)

The detected acoustic wave is a result of its source and medium propagation. The signal frequency is source dependent, which in this case consists of the pressure shock wave generated by the refrigerant gas phase expanding against the gel. The signal amplitudes and time constants, however, relate directly to the medium properties, and should vary accordingly. In consequence, the selected observables consisted of the number of event numbers, amplitudes, time constants and frequencies.

All results were normalized to the refrigerant mass of the SDD. The lines presented in the figures are the best fits to the data, without benefit of theoretical prejudice.

3.1. Ageing

Previously, the detectors were stored at temperatures below 0 °C before they were used, in order to reduce their sensitivity during transport. This test was effected to explore the possible response difference between old and fresh devices, since the lifetime of a superheated droplet detector is limited by the fracture of the gel matrix due to the bubble growth in time because of Oswald ripening [20].

Both SDDs were standard test devices, of a similar constitution: the "fresh" detector had 2.5 g of CCl_2F_2; the "old", 3.9 g of CCl_2F_2. The "old" SDD was kept for 60 days in a freezer at −35 °C; it was defrosted for 3 h prior to measurement. Following defrosting, the "old" SDD gel exhibited a different color and consistency than that of the standard "fresh" one.

There was no significant difference between the two in terms of noise levels, which were generally on the order of 5 mV. The nucleation numbers are generally ~2 times higher with the "fresh" detector, as seen in Fig. 5, which is somewhat unexpected considering the higher refrigerant mass of the "old" device.

As shown in Fig. 6, the "old" detector produced larger signal amplitudes than the "fresh". The signal time constants, shown in Fig. 7, have a similar behavior with temperature, but are 40% larger for the "old" detector, with values characteristic of fractures. The time constants of the "fresh" device are, in contrast, within the range of true nucleation events (Table 1).

The frequency variation with temperature is shown in Fig. 8. The fresh detector response gave a single frequency between 450 and 750 Hz depending on the temperature, whereas the old detector produced a flat ~30 Hz throughout the entire temperature increase. The "old" detector frequency results are characteristic of fractures (Table 1), consistent with the observed time constants. This may explain the much larger amplitudes, since a rupture of the gel produces look-alike events but with much larger amplitude.

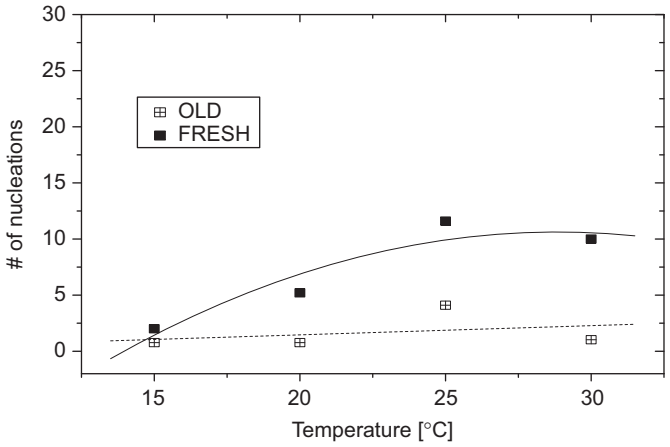

Fig. 5. Variation in signal numbers in terms of detector age and storage.

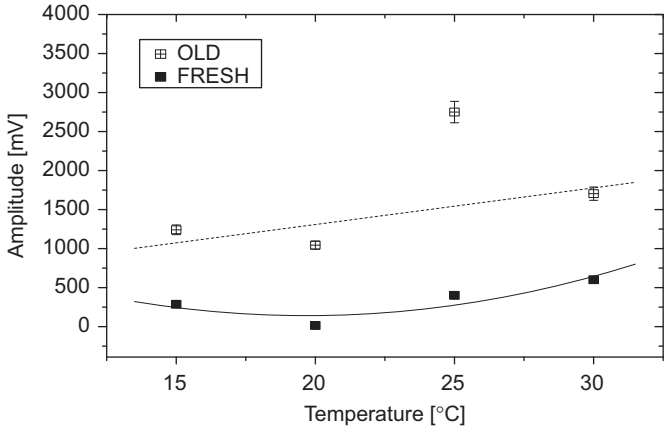

Fig. 6. Variation in signal amplitudes in terms of detector age and storage.

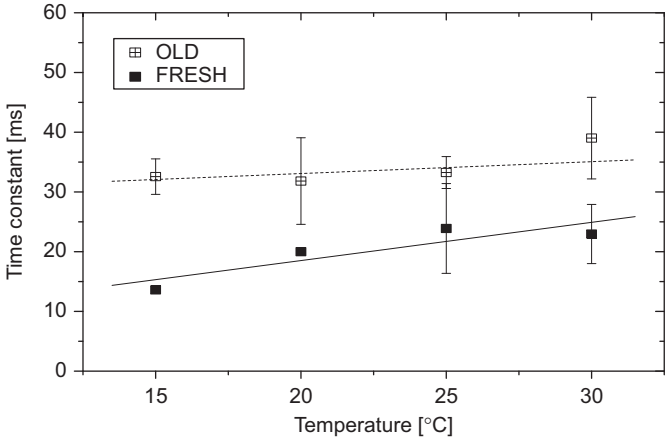

Fig. 7. Variation in signal time constants in terms of detector age and storage.

3.2. Volume/concentration

Two different detector volumes were employed: an 80 ml and a standard (150 ml). Both had a similar uniform dispersion (standard, 2.5 g; 80 ml, 3.0 g) of superheated CCl_2F_2 droplets suspended in an identical gel, corresponding to filling factors of 1.7% and 3.8% respectively.

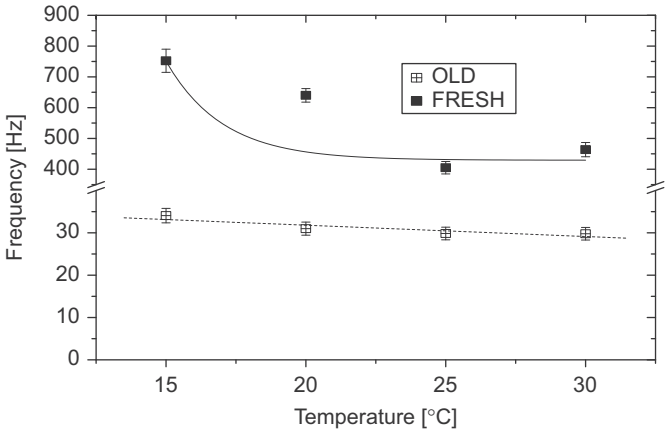

Fig. 8. Variation in signal frequencies in terms of detector age and storage.

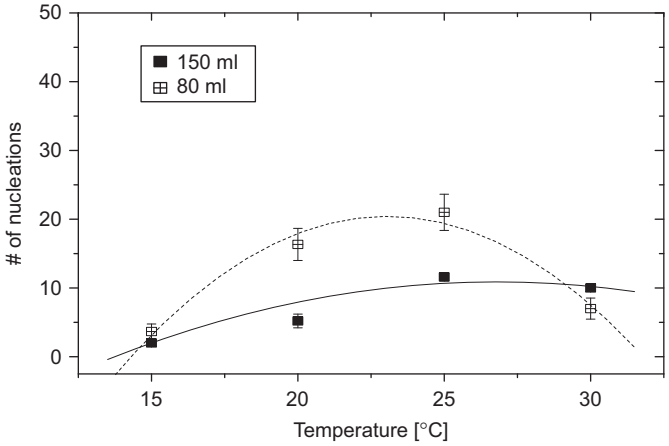

Fig. 9. Variation in signal numbers for the two detector concentrations.

The noise levels of the two detectors were again of order 5 mV, with the noise slightly higher for the smaller SDD, and independent of temperature to within experimental uncertainties.

The number of nucleation events is seen in Fig. 9 to be slightly larger for the smaller volume detector at temperatures below 25 °C, although their behavior is more or less the same with temperature increase. Differences might be the result of the concentration increase, since the small volume concentration is ~50% higher.

In general the signal amplitudes, shown in Fig. 10, increase with temperature as expected for a gel medium increasingly less solid. As anticipated, the amplitudes are larger in the small volume detector than in the standard device. For the standard detector, the amplitudes are low and never rise above 1 V; for the smaller volume device, they begin around 2.5 V at 15 °C and continue to rise in a linear fashion up to 30 °C. This is likely due to less signal attenuation, since there was approximately half of the gel medium in the smaller device.

The time constants of the nucleation signals, shown in Fig. 11, appear slightly dependent on the volume of the SDD, with those of the smaller volume device around 10–15 ms larger.

The frequency response of the two detectors is shown in Fig. 12. Only a single principal frequency between 450 and 750 Hz is observed in the larger volume detector at each temperature. For the smaller volume device, the frequency is essentially constant at ~600 Hz.

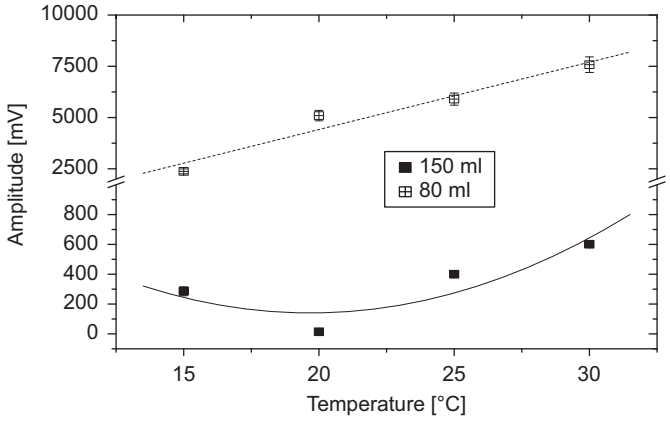

Fig. 10. Variation in signal amplitudes for the two detector concentrations.

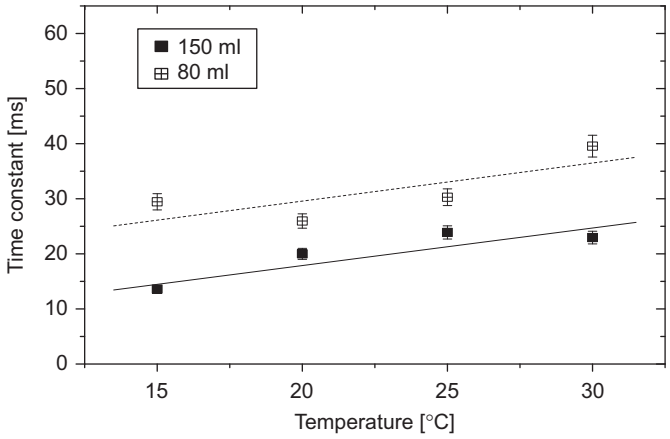

Fig. 11. Variation in signal time constants for the two detector concentrations.

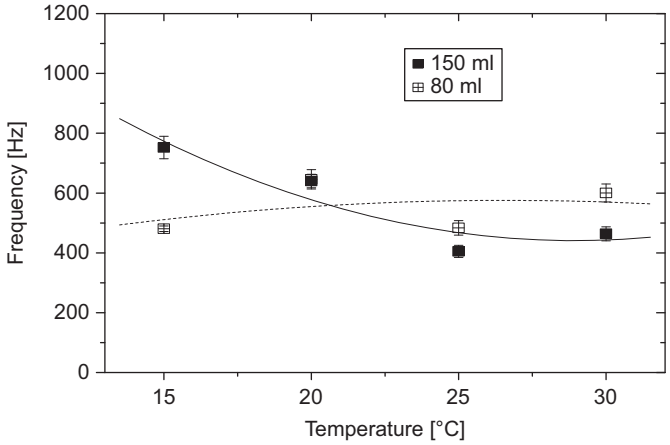

Fig. 12. Variation in signal frequencies for the two detector concentrations.

3.3. Gel composition/stiffness

These tests examined the microphone response to changes in the medium stiffness. Two additional 150 ml detectors were produced for this study using the basic standard recipe, each having the same uniform dispersion of 3.0 g of superheated of CCl_2F_2 droplets, but differing in gelatine concentration: $<$STIFF had 50% less gelatine than a standard SDD; $>$STIFF, 50% more.

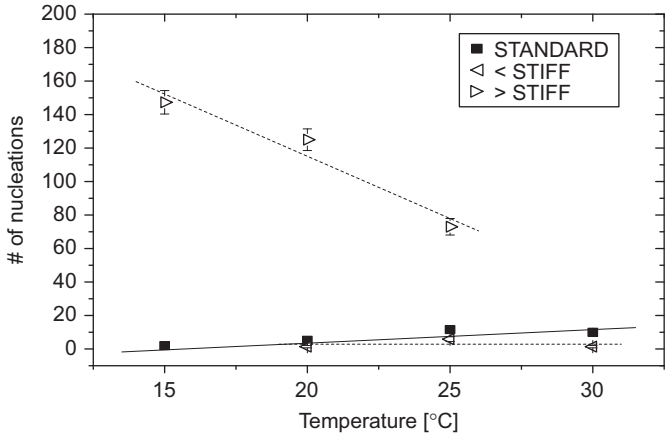

Fig. 13. Variation in signal numbers for the different detector gel stiffness.

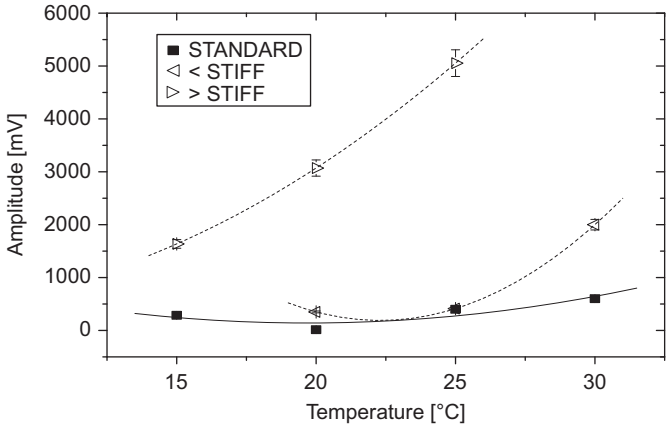

Fig. 14. Variation in signal amplitudes for the different detector gel stiffness.

As seen in Fig. 13, there are significantly more nucleation signals in the $>$STIFF detector, suggesting a possible "sympathetic nucleation" of nearest neighbors; the device in fact was spontaneously bubbling on removal from the hyperbaric chamber.

At 25 °C, due to the massive nucleation rate, the $>$STIFF detector was decomposing and no longer serviceable. In contrast, the $<$STIFF detector did not respond at the lowest temperature. The numbers of nucleation signals in the $<$STIFF detector are slightly less than the standard SDD.

The signal amplitudes of the three detectors (Fig. 14) all display some increase with temperature. The higher amplitudes for the $>$STIFF detector are consistent with a stiffer gel medium absorbing the acoustic shock waves less.

As seen in Fig. 15, all time constants behave similarly, with the lowest value recorded for the $>$STIFF. As the $<$STIFF gel is more relaxed, the time constants are generally larger. All time constants generally increase with temperature.

Fig. 16 shows the recorded signal frequencies. All tend to decrease with increase in temperature, with the standard detector single frequency remaining more or less unchanged, except at the highest temperatures.

3.4. Droplet size

The distribution of droplet sizes depends on the method of preparation of the SDDs [21]. In the process of emulsification of a standard device, where the sensitive liquid is stirred or sheared in

the gel medium to form droplets and then superheated by decreasing the pressure to atmosphere, there is a distribution of diameters formed (40% of 30 μm, 5% of 10 μm and 5% of 60 μm). Given this, a study was made to see if the size of the droplets yields differences in the instrument response.

Two SDDs were made for this study in addition to a standard. The first one, > DROP, had half the normal time (6 h) of stirring and half (150 rpm) the normal shearing for a standard SDD, and therefore a distribution of bigger droplets (60 μm—40%). The second, < DROP, had twice the normal stirring time (12 h) and the same 300 rpm of the normal shearing for a standard SDD; it had a

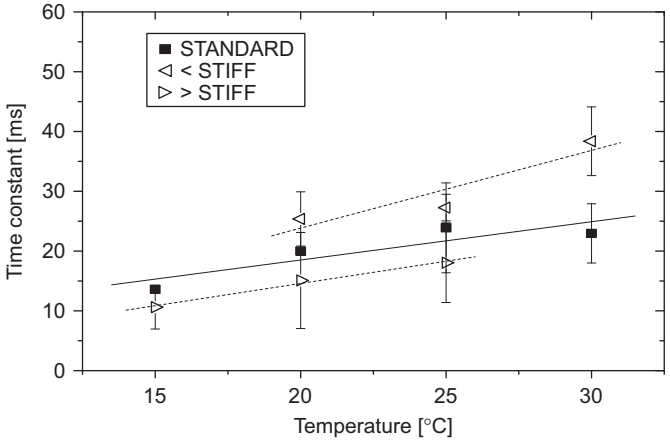

Fig. 15. Variation in signal time constants for the different detector gel stiffness.

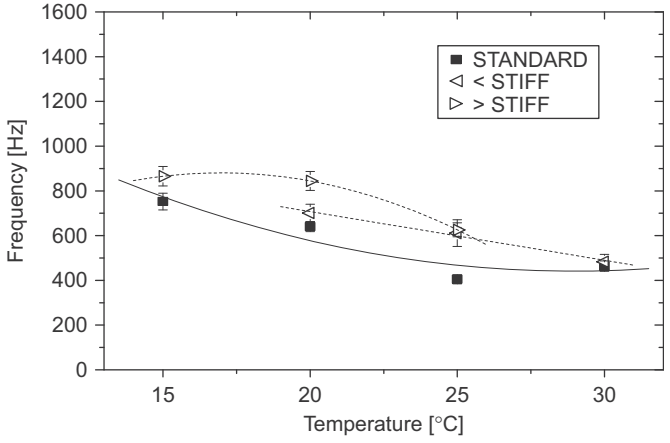

Fig. 16. Variation in signal frequencies for the different detector gel stiffness.

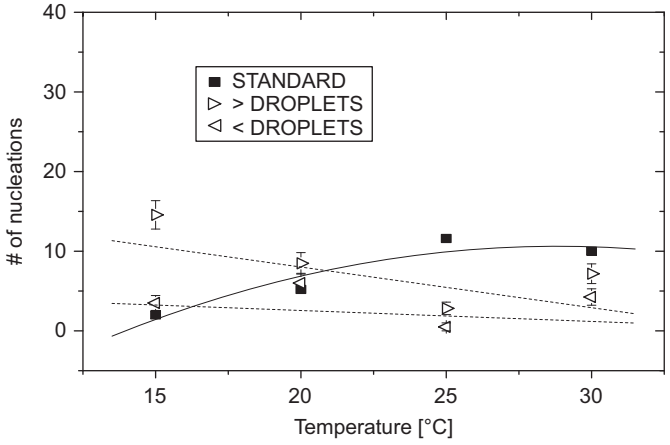

Fig. 17. Variation in signal numbers for detectors with different droplet size.

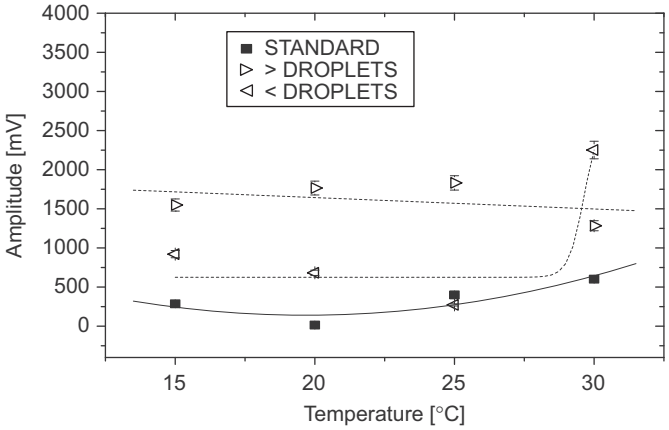

Fig. 18. Variation in signal amplitudes for detectors with different droplet size.

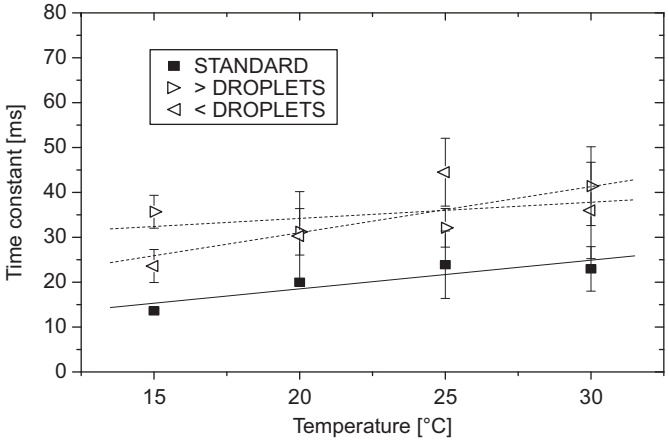

Fig. 19. Variation in signal time constants for detectors with different droplet size.

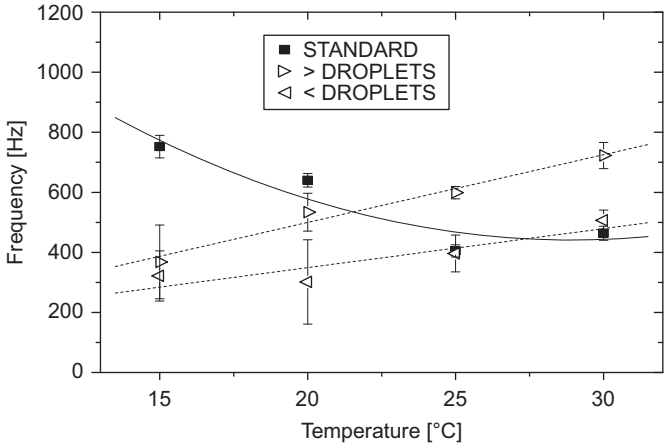

Fig. 20. Variation in signal response frequencies for detectors with different droplet size.

distribution of smaller droplets (10 μm—40%). This was confirmed visually for both detectors. All detectors otherwise had similar constructions: the $<$DROP detector had 4.6 g of CCl_2F_2; the $>$DROP, 4.0 g and the standard normal, 2.5 g.

The noise levels for all detectors were similar at ~5 mV, with the $>$DROP about 1.5 × larger than the others. The nucleation signal numbers, shown in Fig. 17, are similarly about the same despite that the $>$DROP detector has more events at the beginning of the test at 15 °C.

As shown in Fig. 18, the signal amplitudes for the $>$DROP detector are 1.5–3 larger than the others, which is possibly related to the ~50% larger size of the droplets. The $<$DROP and standard devices generally behave similarly.

The behavior of the signal time constants for the three detectors (Fig. 19) is essentially the same throughout the measurements. Both SDDs with droplet size variations exhibit signals with time constants of 20–40 ms, whereas those of the standard SDD are always between 10 and 20 ms.

As seen in Fig. 20, both the $<$DROP and $>$DROP detectors showed an approximately linear increase of signal frequency with temperature, whereas the standard signal appears to asymptotically decrease to ~500 Hz.

4. Discussion

The noise levels observed in all SDD trials are generally low (5 mV), and reflect the use of the new microphone-based electronics. A complete power spectrum analysis of the experiment signals was performed, yielding the acoustic event percentages for each of the tests as indicated in Table 2. No microleaks were observed in the studies since the devices were not pressurized. The fracture percentage is insignificant for all detectors, with the exception of the "old" detector which consisted of ~100% fractures due to the deterioration of the gel. In the majority of the detectors, less than 1% of the events were identified with trapped gas (N_2), the exception being the $<$STIFF.

4.1. Device ageing

The gelatin gels at temperature below 30 °C by association of three polyelectrolyte chains into a triple helix conformation [22]. Frozen gel is not in an equilibrium state: for storage times $>$12 h, the lower temperature catalyzes the process of gelification and helices continue to be formed very slowly in time, increasing the viscoelasticity of the gel.

The freezing of the SDD also reduces the droplet size, as the Freon continues to dissolve into the gel [22]; the lower the temperature, the more soluble is the detector. The nucleation rate of the "old" detector shows indeed a lower rate than expected and moreover a flat response. In comparison, the curves from $<$DROPLET and the "old" detectors exhibit more or less the same low counting rate.

Following the measurements with the "old" SDD, optical microscopy of the stored "old" SDD identified a significant presence of clathrate hydrates at low temperature, which tend to "glitter" because of the ice crystal cages encrusting the droplets. Clathrate hydrates are crystalline, water-based solids physically resembling ice, in which small non-polar molecules (typically gases) are trapped inside "cages" of hydrogen bonded water molecules. Their formation and decomposition are first-order phase transitions and not chemical reactions; they are not chemical compounds since the caged molecules are not bonded to the lattice. The clathrate hydrates surrounding the droplets break the metastability as a mechanical action independent of temperature, as if the droplets are "pierced" by the clathrate hydrates and then nucleate.

By comparing the frequency curves of $<$DROPLET and "old" SDDs, it is seen that the signal frequencies are not the same. The clathrate hydrates surround the droplets like a cage, changing the frequency and rupturing the gel. The flat frequency and event rate curves with temperature increase evidence the mechanical effect of the clathrate hydrate presence. Their presence implies that the device cannot be stored in a stable liquid phase at temperatures below 0 °C because clathrate hydrates provoke spontaneous nucleation locally on the droplet surfaces when warming to room temperature, altering significantly the event frequencies and eventually destroying the device.

4.2. Temperature variation

The signal frequency is source dependent, which in this case is determined by the pressure shock wave generated by the rapid expansion of the refrigerant gas phase against the gel. As the gel becomes "softer" with increasing temperature, hence less resistant to the expansion, a general decrease in frequency with increasing temperature is to be expected. The source however being a shock wave, there will be an associated disturbance of the gel in its immediate vicinity and effects on the initial wave propagation.

Experimentally, a virtually constant frequency of 400–800 Hz is observed throughout the various experiments, with a tendency to decrease with temperature which can be attributed to the gel softening. The exception is in the variations of droplet size, in which the reverse is seen.

Both the signal amplitudes and time constants are measures of the gel elasticity. The pressure amplitude (p) is given by $p=k\rho_0 v^2 A_m$, where k is the wave number, ρ_0 is the initial pressure, A_m is the maximum amplitude, and $v=[B/\rho_0]^{1/2}$, with B the gel bulk modulus. Although v decreases with temperature increase [23], the increasing gel softness with higher temperatures permits an increase in A_m. Accordingly, both in principle increase with increase of temperature as the gel tension relaxes. Experimentally, apart from small variations, the time constants are essentially constant or slightly increased throughout the study, indicating a virtually unchanged gel consistency over the temperature range of these measurements. The signal amplitudes of the various variations all tend to increase with temperature, as expected.

In general, the sensitivity (number of nucleations) of the SDDs also increases with temperature, since temperature increase raises the degree of superheat, lowering the energy threshold required for bubble nucleation. The CCl_2F_2 reduced superheat at 30 °C and 1 bar is however 0.42, well below the $s=0.5$ onset of SDD sensitivity to electrons, muons, γ's and other minimum ionizing radiations, so that the observed general increase in number of

Table 2
Acoustic background events in each of the experiments (percentage of total events).

Acoustic backgrounds	Standard	Old	80 ml (higher concentration)	$<$STIFF	$>$STIFF	$<$DROP	$>$DROP
Trapped N_2	0.8	1	0.3	3.4	0	1.1	1
Fractures	0	99	0	0	0.4	0.4	0.9

nucleation events cannot be a related result. Larger droplets might also produce a larger numbers of higher amplitude events due to their larger geometrical cross-section.

4.3. Fabrication variations

As in the temperature variation, there are no significant differences in either the recorded frequencies or signal time constants, although both tend to be slightly larger than a standard device. Larger amplitude signals are generally observed in the increased refrigerant concentration, stiffer gel and larger droplet sizes.

4.3.1. Concentration variation

A higher refrigerant concentration implies a decrease in the mean inter-droplet distance, and an increase in the probability of sympathetic nucleation of nearby droplet neighbors. In principle, this leads to a superposition of nucleations and an effective increase in the recorded amplitude. Beyond the increased density of acoustic scattering sites, there is no significant change in the medium and the signal propagation should result in essentially unchanged time constants and frequencies.

Experimentally, the signal amplitude of the higher concentration device is $\sim 10\times$ larger than that of a standard device, with a uniformly increased signal time constant and a generally constant frequency of ~ 600 Hz. The increased 3.8% concentration of the smaller device remains well-below the $\sim 14\%$ percolation threshold of SDDs [24].

The increased concentration also has an impact on the droplet size distribution, which increases, because the droplets coagulate as a result of the saturation of the liquid Freon in the liquid gel during SDD fabrication. Comparing the $>$DROPLET and 80 ml results, we have the same behavior for Figs. 10, 12, 18 and 20. The event rate behavior seems the same with a decrease in temperature, due to the larger droplets initially having a higher vaporization probability.

4.3.2. Gel stiffness

A less elastic gel also implies an increase in the probability of sympathetic nucleations and an effective increase in the recorded signal amplitude, which is evidenced in the observed numbers of nucleation events prior its self-destruction at 30 °C.

From polarimetry measurements, the rate of helix formation $\chi=0.55$ [20]. Since the helix concentration is $c_{\mathrm{helix}}=\chi c_{\mathrm{gel}}$ [22,25], we have for the standard gel $c_{\mathrm{helix}}=9.68\times 10^{-3}$ and $1.94\times 10^{-2}\,\mathrm{g\,cm^{-2}}$ for the $>$STIFF. The modulus is given by $B=(2.1\times 10^{9})c_{\mathrm{helix}}^{2}$ [17,20], so that the ratio is $B_{>\mathrm{STIFF}}/B_{\mathrm{standard}}=121$: by adding 50% more gel (3.52% instead of 1.76%), the gel's stiffness was increased by a factor 100. The nucleation rate is high in the case of the $>$STIFF, since the droplets are compressed by the gel media: in consequence the radiation-induced nucleation event rate is masked by the stiffness effect. The nucleation rate of the $>$STIFF device decreases with temperature increase because the stiffness of the gel also decreases. Moreover, as the temperature increases, the viscoelasticity of the gel is lowered since there is a decrease in the helix amount and the gel is becoming more liquid: the droplets are increasingly less compressed and the event rate decreases, reaching a "normal" rate where the radiation-induced nucleations dominate.

An increased gel stiffness also implies less energy dissipation, and generally smaller signal time constants. Since the refrigerant gas bubble must encounter an increased resistance in expanding against the gel, it seems likely that a stiffer gel should yield slightly higher frequency signals.

Experimentally, the signal amplitudes of the $>$STIFF device are $\sim 10\times$ larger than those of a standard device, with time constants slightly lower and frequencies slightly larger at the lower temperatures than the standard. For the $<$STIFF device, the frequency and amplitude are generally those of the standard, with the time constant slightly higher than the standard.

4.3.3. Droplet size variations

Larger droplets should expand more (order $10\times$) than smaller droplets, with an accompanying increase in the signal amplitudes. They also imply an increase in the probability of sympathetic nucleations, and further increase in the recorded signal amplitude. It also seems likely that larger droplets will expand more rapidly than the smaller for the same gel conditions, generating a higher frequency pressure pulse as observed. Given that the gel is for the most part unchanged however, the pulse dissipation should be relatively unchanged and the time constants more or less constant.

It might be expected that larger droplets scatter the shock wave more, which should lead to an amplitude loss and some frequency dispersion—neither of which is however observed.

Experimentally, the signal amplitudes associated with the large droplet device are uniformly $\sim 4\times$ those of the standard, while the small droplet amplitudes are $\sim 2\times$. Both time constants are slightly larger than the standard device, with the larger droplet device larger than the smaller at lowest temperatures. The recorded frequencies are initially smaller than the standard, with the larger droplets larger than the smaller.

As previously noted in Section 4.1 above, an increased concentration also leads to an increase in the distribution of droplet size, so that the behavior of the $>$DROPLET and 80 ml devices is similar.

5. Conclusions

We have examined the response of SDDs to variations in the standard chemistry of their fabrication which have impact on both the acoustic source and propagation medium, as well as the SDD lifetime. The results are in general agreement with what might be expected from considerations of both the bubble nucleation and gel medium properties, and show that normal small fabrication variations have a relatively small influence on detector performance.

In terms of detector design, a device providing a temperature-independent amplitude, fast-falling signal pulse with an essentially constant primary response frequency is to be desired. With these criteria, the results suggest that SDD fabrications other than the standard one are not to be preferred, although minor alterations can be consciously made in order to achieve certain particular results. For instance, the larger droplet results are of particular interest following the recent observation by PICASSO [26] of the possibility to discriminate α from neutron events on the basis of their differing pulse amplitudes, following an increase in their droplet sizes to $\sim 200\,\mu$m diameters.

The storage of detectors below 0 °C following fabrications is in all cases clearly to be avoided.

Acknowledgments

We thank the Portuguese Research Reactor crew for their many contributions to these measurements. The work of M. Felizardo was supported by POCI grants FIS/55930/2004, FIS/57834/2004 and PTDC/FIS/83424/2006 of the Portuguese Foundation for Science and Technology (FCT); the activity was also supported in part by POCI grant FP/63407/2005 of the CERN Program of FCT, co-financed by FEDER.

References

[1] R.E. Apfel, Nucl. Instr. and Meth. 162 (1979) 603.
[2] F. Seitz, Phys. Fluids 1 (1958) 2.
[3] H.W. Bonin, G.R. Desnoyers, T. Cousins, Radiat. Prot. Dosim. 46 (2001) 265.
[4] BTI-Bubble Technology Industries, 〈http://www.bubbletech.ca〉.
[5] F. d'Errico, W.G. Alberts, G. Curzio, et al., Radiat. Prot. Dosim. 61 (1995) 59.
[6] F. d'Errico, A. Prokofiev, A. Sanniko, H. Schuhmacher, Nucl. Instr. and Meth. A 505 (2003) 50.
[7] T.A. Girard, F. Giuliani, J.I. Collar, et al., Phys. Lett. B 621 (2005) 233.
[8] M. Barnabé-Heider, M. Di Marco, P. Doane, et al., Phys. Lett. B 624 (2005) 186.
[9] F. d'Errico, Nucl. Instr. and Meth. B 184 (2001) 229.
[10] H. Ing, H.C. Birnboim, Nucl. Tracks Radiat. Meas. 8 (1984) 285.
[11] P. Berkvens, P. Colomp, Radiat. Prot. Dosim. 120 (2006) 509.
[12] M. Das, B.K. Chatterjee, B. Roy, S.C. Roy, Phys. Rev. E 62 (2000) 5843.
[13] M. Das, B.K. Chatterjee, et al., Nucl. Instr. and Meth. A 452 (2000) 273.
[14] B. Roy, B.K. Chatterjee, M. Das, S.C. Roy, Radiat. Phys. Chem. 51 (1998) 473.
[15] M. Barnabe-Heider, M. DiMarco, P. Doane, et al., Nucl. Instr. and Meth. A 555 (2005) 184.
[16] M. Felizardo, R.C. Martins, A.R. Ramos, et al., Nucl. Instr. and Meth. A 589 (2008) 72.
[17] J.I. Collar, J. Puibasset, T.A. Girard, et al., New J. Phys. 2 (2000) 14.
[18] F. Giuliani, C. Oliveira, J.I. Collar, et al., Nucl. Instr. and Meth. A 526 (2004) 348.
[19] M. Felizardo, R.C. Martins, T.A. Girard, et al., Nucl. Instr. and Meth. A 585 (2008) 61.
[20] T. Morlat, D. Limagne, G. Waysand, et al., Nucl. Instr. and Meth. A 560 (2006) 339.
[21] R. Sarkar, B.K. Charterjee, B. Roy, S.C. Roy, Radiat. Phys. Chem. 71 (2004) 735.
[22] T. Morlat, Ph.D. Thesis, University of Paris 6, 2004, unpublished.
[23] M. Felizardo, R. Martins, T.A. Girard, et al., Nucl. Instr. and Meth. A 599 (2009) 93.
[24] J. Puibasset, Ph.D. Thesis, University of Paris 6, 2000, unpublished.
[25] C. Joly-Duhamel, D. Hellio, A. Ajdari, M. Djabouov, Langmuir 18 (2002) 7158.
[26] F. Aubin, M. Auger, M.-H. Genest, et al., New J. Phys. 10 (2008) 103017.